



## Curve Skeletons of Planar Domains

Ata A. Eftekharian<sup>1</sup> and Horea T. Ilies<sup>2</sup>

<sup>1</sup> University of Connecticut, [eftekharian@engr.uconn.edu](mailto:eftekharian@engr.uconn.edu)

<sup>2</sup> University of Connecticut, [ilies@engr.uconn.edu](mailto:ilies@engr.uconn.edu)

### ABSTRACT

Curve skeletons are 1D entities that capture the essential topology and geometry of a shape in a simple and very compact form, and have found a multitude of applications in engineering and science. The concept itself is ill-defined, which is why the many existing definitions are ad-hoc and employ heuristic algorithms revolving around the (unique) medial axis. We propose a framework for computing curve skeletons for arbitrary planar domains that relies on a modified medial axis, and is based on R-functions that can be thought of as continuous forms of the Boolean logic functions. Furthermore, we propose one particular definition of such a curve skeleton that preserves the homotopy of the domain, is stable in the presence of noise and is well-suited to downstream applications. The framework can be implemented in any commercial geometric kernel for planar domains, and has attractive computational properties. Furthermore, the mathematical concepts are extendable to medial surfaces and curve skeletons in 3D domains.

**Keywords:** distance functions, medial axis, curve skeletons.

**DOI:** 10.3722/cadaps.2011.87-97

### 1 MOTIVATION

Geometric models are becoming ubiquitous in engineering and scientific applications. We have the ability today to construct and manipulate geometric models with an accuracy that satisfies even the most demanding applications. However, the increase in accuracy comes at the expense of an increased model complexity, which, in turn, may impede downstream applications.

Curve skeletons have been defined in an attempt to provide a simple and compact representation of the essential topologic and geometric properties of a shape. However, a curve skeleton is, in general, an ill-defined concept, which has prompted the proposal of a number of ad-hoc definitions discussed in the next section. Curve skeletons are also sometimes known as “centerlines” or “medial curves”, which is why most of the existing definitions revolve around the (well-defined) concept of *medial axis*.

Introduced by Blum [1] as a tool for image analysis, the medial axis has become one of the mainstream geometric concepts due to the fact that it provides a compact representation of the geometric features of a shape and its topology. The medial axis captures the connectivity of the shape, has a lower dimension than the space itself, and is closely related to the distance function constructed over the same domain. The concept of medial axis has been described with the help of the fire grass

concept (see for example [2]) as follows: if a fire starts from all points of a planar curve at the same time and moves with constant velocities in all directions in the same plane, then the medial axis is the locus of points where the fire (in fact a moving front) meets itself. The concept can be extended to  $k$ -dimensional geometric shapes in  $R^k$ , case in which the medial axis becomes a set of dimension  $k-1$ . Intuitively, the points on the medial axis are equally distant to at least two points of the boundary of the domain.

### 1.1 Prior Art

Since the curve skeleton is assumed to be in the “middle” of a shape, most definitions relate the curve skeleton to a subset of Blum's medial axis. Therefore, it should not be surprising that most algorithms that compute curve skeletons use a procedural variation of the medial axis algorithms. A good review of the state of the art and the limitations of current algorithms for medial axis computation appears in [2], while a survey of the many applications of curve skeletons is provided in [3] along with a detailed discussion of the desired properties of such representations. Essentially, the current algorithms for curve skeleton computations employ either: thinning algorithms, which implement some versions of the fire grass concept such as [4, 5, and 6]; distance functions and Voronoi decompositions [7, 8, 9, 10, and 11]; level sets [12]; or potential fields [13, 14].

Various approximations of symmetry axes that are used to extract curve skeletons for tubular shapes are discussed in [15, 16]. An automatic centerline extraction is discussed in [17], which computes first the medial axis followed by a pruning step to obtain “well centered” paths. The user defines two (extreme) points on the medial axis, which is followed by running a shortest path algorithm between the two points of the medial axis whose output is the computed centerline. They also propose to prune the medial surface by removing all branches connected to end-points and whose lengths are lower than a specified threshold. Guaranteeing that the centerline will be located in the “middle” of the object everywhere, as well as handling domains with holes and establishing connectivity of the centerline to the boundary may be problematic. A new approach that defines the curve skeleton of 3D solid shapes as the critical points of a geodesic distance function on the medial axis has been proposed in [18]. Their algorithm computes the curve-skeleton by eroding the medial axis, and is stable in the presence of noise even though the corresponding medial axis may be unstable. A number of papers have discussed specific applications of curve skeletons in virtual endoscopy [17, 19], shape segmentation [20], dimensional reduction in boundary value problems [21, 22], shape similarity [23], virtual navigation [24].

### 1.2 Scope and Outline

We have proposed in [25] a novel framework for computing the medial axis of a planar domain by constructing the exact distance function with R-functions that operate on the real valued halfspaces bounding the domain as logic operators. The medial axis is extracted from the distance function as the projection of its ridges, where the distance function is not differentiable (note that there are other points of the distance function where it is not differentiable, namely the ravines. By extracting both ridges and ravines of the distance function, one obtains a superset of the medial axis [25]). In this paper we show how to modify this framework to compute curve skeletons for arbitrary planar domains. Furthermore, we propose one specific modification of the distance function which results in a skeleton that:

- is a curve skeleton that is homeomorphic to the medial axis and hence it preserves the homotopy of the domain;
- relies on formalism that is extendable to 3D domains, and
- has attractive computational properties, including the computability by using standard algorithms within existing commercial CAD systems.

## 2 CONSTRUCTING THE DISTANCE FUNCTION OVER THE DOMAIN

Assume that the planar domain is a closed, bounded, regular and semi-analytic pointset  $\Omega$ , i.e., described by real-function inequalities, or halfspaces,  $f_i \geq 0$ . We adopt the convention that each  $f_i$  is positive inside the domain  $\Omega$ , and negative outside. Clearly,  $f_i = 0$  on the boundary  $\partial\Omega$  of  $\Omega$ . Furthermore, the Euclidean distance to the boundary of every such domain  $\Omega$  is usually defined as

$$d(p) = \inf \| p - x \|_{x \in \partial\Omega}$$

Each halfspace  $f_i(x, y)$  induces a higher dimensional halfspace in the  $(x, y, f(x, y))$  space denoted by

$$H_i \equiv H_i(x, y, f_i(x, y)) \geq 0 \quad (1)$$

It is easy to see that, in general, the boundary  $\partial H_i$  of  $H_i \geq 0$  is not a distance function to  $f_i = 0$ . However, such a distance function can be constructed for every  $f_i = 0$  either exactly (analytically) or approximately [26, 27], and therefore for the remainder of this paper we assume that  $\partial H_i$  is the distance function to curve  $f_i = 0$ .

One of the main consequences of the theory of R-functions invented by Rvachev [28] is that one can obtain one single real function inequality  $\omega \geq 0$  for any closed, bounded, regular and semi-analytic geometric shape  $\Omega$  bounded by primitive sets, or function inequalities,  $f_i \geq 0$ . Function  $\omega$  is obtained by first constructing an appropriate R-function predicate using the usual logical functions, and substitute its arguments with the functions describing the primitive sets  $f_i \geq 0$ . The resulting function  $\omega$  is continuous over domain  $\Omega$ , has known differential properties, and its zero level set is the domain  $\Omega$  itself. If  $\partial H_i$  are distance functions to  $f_i = 0$ , i.e.,  $f_i(x, y) = d(p(x, y))|_{f_i=0}$ , then we can substitute  $H_i$  instead of  $f_i$  in the R-function expression to obtain the exact distance function over  $\Omega$ .

Conceptually, the problem of constructing a Boolean expression for a domain bounded by halfspaces is the same as that of converting a Boundary Representation (B-rep) into a Constructive Solid Geometry (CSG) representation in Solid Modeling [29]. The Boolean set representation of a polygonal domain can be computed based on the Convex Deficiency Tree [30], which treats each polygon as its convex hull minus a finite number of concavities. Note that the polygon is a closed set, so the subtraction of concavities must necessarily be regularized (i.e., one must use regularized Boolean operations). Importantly, this construction algorithm for simple polygons can be extended to some other point sets, such as curved polygons [31], 3D polyhedra, and more general 3D solids [32, 33].

By performing the syntactic substitution mentioned above, we obtain a function  $\omega$  that is the exact distance function for any convex planar domain, and an approximate distance function for a concave domain. Note that such a distance function is obtained from the principal system of R-functions [25]

$$R_\alpha(\Delta) : \quad \frac{1}{1+\alpha} \left( x_1 + x_2 \pm \sqrt{x_1^2 + x_2^2 - 2\alpha x_1 x_2} \right) \quad (2)$$

by setting the value of  $\alpha = 1$ , i.e., the  $R_1(\Delta)$  system. Values of  $\alpha < 1$  correspond to R-functions over the same domain that have established differential properties [29]. The approximate distance functions obtained from  $R_1(\Delta)$  can be converted into exact distance functions by introducing additional

halfspaces at the concave vertices of the domain. Specifically, each concave vertex requires a conical halfspace with a half angle of  $\pi/4$  and two separating/trimming halfspaces that are normal to the boundary curves that are incident at the concave vertex. In practice, we add trimmed conical halfspaces to all vertices of the domain, which eliminates the need to keep track of the domain convexity because a trimmed conical halfspace will contribute to the resulting function only when the corresponding vertex becomes concave [25].

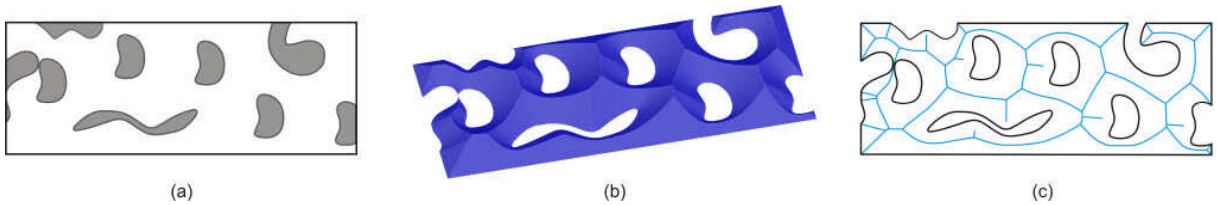


Fig. 1: A planar domain (a), its distance function (b) and the projection of the ridges of the distance function onto the plane of the domain (c).

### 3 CURVE SKELETONS

We identify in the medial axis  $MA(\Omega)$  three types of points illustrated in Figure 2:

- junction (or branch) points - where three or more branches of the medial axis meet, or, alternatively, where the maximal disc has three or more contact points with the boundary of the domain;
- convex end-points - these points are both points of the medial axis as well as convex corners of the original domain  $\Omega$ ;
- free-end-points - end-points of the medial axis that are NOT on the boundary of the original domain  $\Omega$ ;

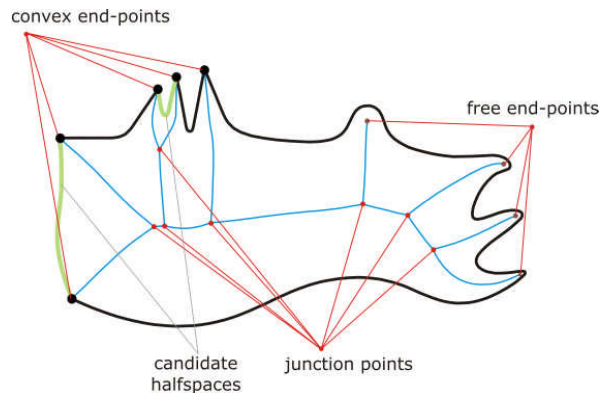


Fig. 2: The three types of medial axis points.

It is known that the number of junction points for any semi-analytic domain is finite [34, 35] and that these junction points can be used to decompose the original domain into “primitive” subdomains whose medial axis transforms are piecewise real analytic curves, i.e., the so called “fundamental domains” [34]. It follows that the maximal ball centered at any point of the medial axis that lies between two junction points or between a junction point and an end-point (convex or free as defined above) will have exactly two contact points with the boundary of the planar domain. These medial axis points are also known as normal points, and all branches of planar solid domains that are

bounded by two junction points contain only normal points in the interior. Furthermore, the convex and free end-points will bound branches of the medial axes that do not connect to any other branches of  $MA(\Omega)$  at those end-points.




	junction	convex	free
junction	See Fig 2	See Fig 2	See Fig 2
convex			
free			

Fig. 3: Branch taxonomy based on branch end-points. Only the upper half of this matrix is populated due to its symmetry.

The branches of the medial axis can be classified based on their endpoints as shown in Figure 3. The branches whose end-points are both junction points connect to other branches at both ends and therefore this type of branches can be found in essentially every type of curve skeleton that has ever been proposed. These branches capture the topology of the domain - see for example Figure 1, and therefore they will not be modified. Furthermore, the branches whose end-points are of the same type (i.e., either both convex or both free end-points) come from shapes whose medial axis consists only of one branch as illustrated in Figure 3 so these will be preserved. Hence, it is reasonable to expect that the only branches of the medial axis that can potentially be modified or pruned would be those that have a junction point at one end and either a convex or a free end-point at the other end.

By modifying the distance functions corresponding to some of these candidate branches, and by substituting these modified distance functions in the Boolean expression computed as described above, we obtain a new continuous function  $\omega^m$  over  $\Omega$ , whose ridges can be projected onto the plane of  $\Omega$  to obtain the curve skeleton. Once the candidate branches have been identified, one needs to: (1) identify the corresponding halfspaces  $f_i$  that generate each such branch; (2) modify the corresponding distance functions  $H_i$ ; (3) recompute the projections of the new ridges of the continuous function  $\omega^m$  that form the curve skeleton; and (4) prune the branches that are coincident with the boundary of  $\Omega$  as well as a subset of those branches that are bounded by one junction point and either a convex or a free end-point. One specific choice is proposed in the next section.

Note that this framework supports the formulation of multiple curve skeletons that can be obtained by changing the distance functions that are being modified and the branches that are being pruned.

**3.1 One Particular Curve Skeleton**

One particular type of skeleton that is well suited to a number of practical applications can be obtained by eliminating from the medial all branches that have one junction point at one end; and either a convex or a free end-point at the other end. To this end, the distance functions corresponding to the halfspaces  $f_j$  generating branches bounded by the same junction point and a convex end-point will be modified such that they become perpendicular to the plane of  $\Omega$  at every point along  $f_j = 0$ . Referring to Figure 2, the distance functions corresponding to the halfspace(s) that define the leftmost boundary curve will be modified, which will effectively “push” the leftmost junction point towards the boundary curve. In the example illustrated in Figure 2 there is one other such boundary curve as shown.

If we denote by  $H_j^m$  the modified distance functions, then the  $H_j^m$ 's are substituted in the R-function expression to replace the corresponding  $H_j$ 's. The resulting continuous function is no longer a distance function everywhere, but the projection of its ridges result in a modified skeleton for which specific junction points as well as the end branches bounded by these junction points are on the boundary of  $\Omega$ . Once the new skeleton is recomputed, the skeleton is pruned of all branches (minus the corresponding junction points) that overlap with  $\partial\Omega$  as well as those branches that have a convex or a free end-point at one end.

Figure 4 illustrates these steps for a planar domain bounded by free-form curves. The medial axis  $MA(\Omega)$  is shown in Figure 4(a). There are two candidate distance functions for modification, namely  $H_1$  and  $H_2$  as indicated in the figure because these distance functions create branches that are bounded by the same junction point at one end and by a convex end-point at the other end. In the second step, these distance functions are modified so that they become perpendicular to the plane of  $\Omega$ . The projections of the ridges of the new continuous function  $\omega^m$  are shown in Figure 4(b), which form the modified skeleton. The exact distance function  $\omega$  and the modified function  $\omega^m$  are shown in Figures 4(d) and (e). The final curve skeleton that is obtained as a result of the pruning step is shown in Figure 4(c).

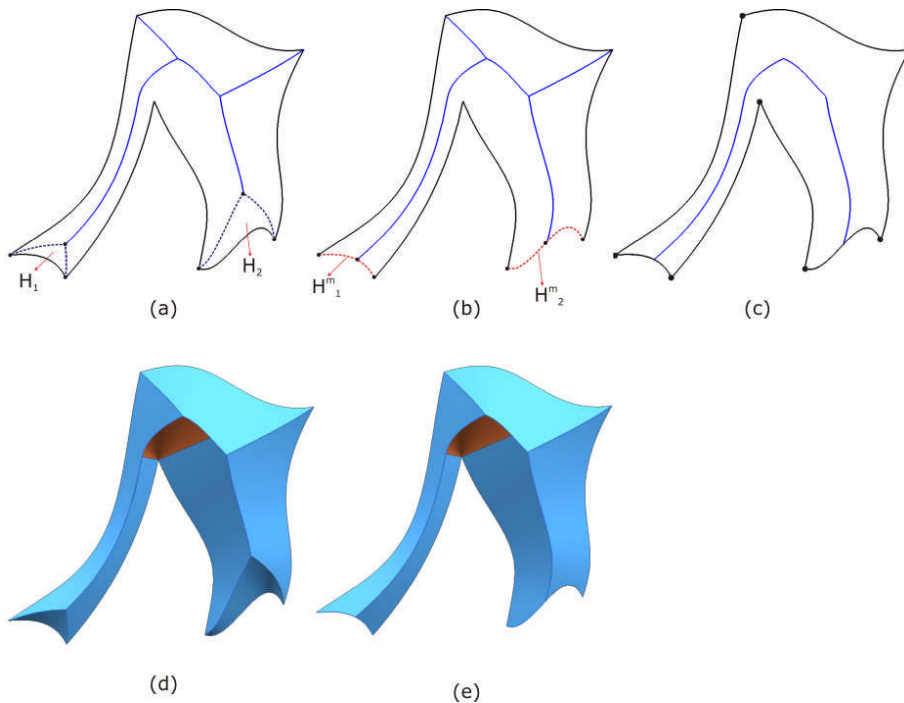


Fig. 4: Medial axis  $MA$ , modified  $MA$  and the curve skeleton after the pruning step for an arbitrary domain.

Our implementation accepts a boundary representation of the domain bounded by free-form boundary curves as input. The distance functions to individual halfspaces are computed either analytically for linear and quadratic halfspaces, or approximately. The ridges are extracted by using discrete Laplacian implementation as discussed in detail in [25]. We compute the neighborhood graph of all points on the medial axis, which is heavily exploited in identifying the three types of points defined above and the corresponding candidate branches.

### 3.2 Singular Cases

For some domains, such as those for which two or more junction points collapse into the same junction point, selecting an appropriate curve skeleton becomes impossible without additional information or heuristics. Such an example is illustrated in Figure 5 where two junction points from (a) collapse into a single junction point (b). This shape clearly admits at least two curve skeletons as illustrated in Figures 5(c) and (d) and selecting one of these possible skeletons requires additional information from the user or heuristics.

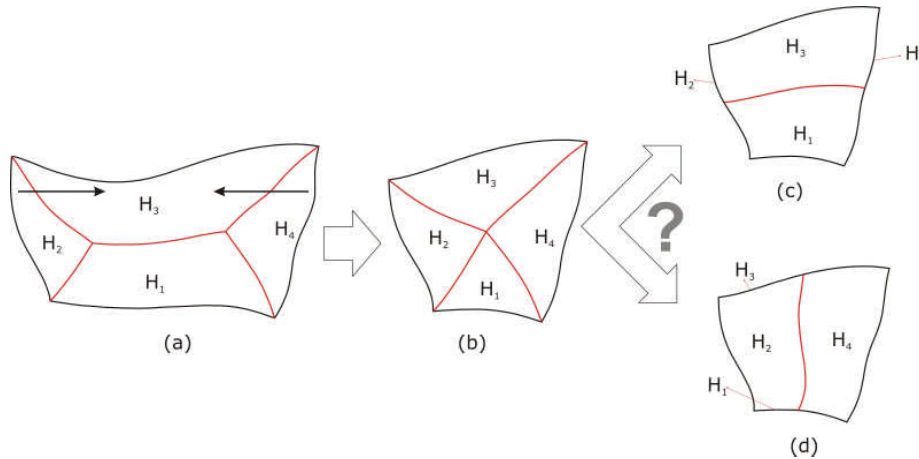


Fig. 5: Medial axis and curve skeleton of an arbitrary domain in a singular case. Deciding which curve skeleton to compute requires heuristics or additional information from the user.

A similar example is illustrated in Figure 6 in which the original medial axis from (a) can be modified to obtain either of the three curve skeletons shown in Figure 6 (b-d). Such a multi-prong junction point can occur in more complex domains such as the one shown in Figure 6 (e) which can lead to either one of the skeletons shown in Figures 6 (f) or (g).

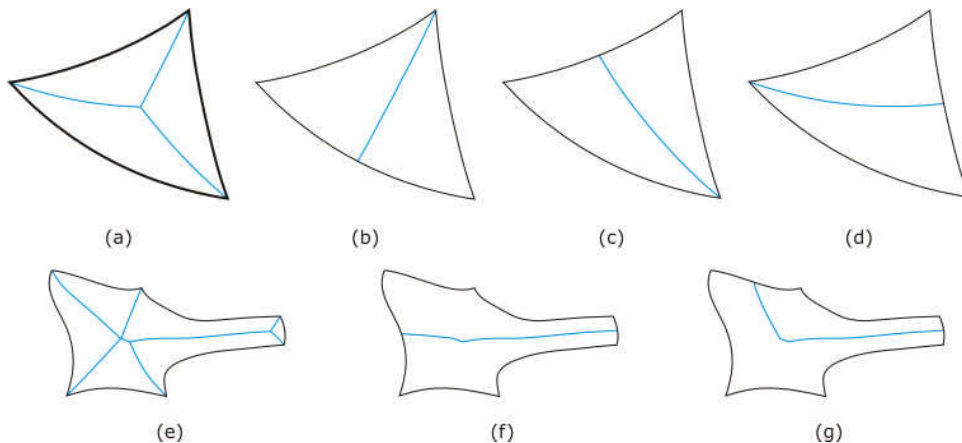


Fig. 6: Medial axis of a topological triangle (a) and three possible curve skeletons (b-d). A more complex domain with a four-prong junction point.

#### 4 EXAMPLES

In this section we illustrate several examples in which branches bounded by a junction point and either a convex or a free end-point are eliminated from the skeleton as described above.

The first two examples illustrate a planar cross-section of a compliant robotic hand without the actuators shown in Figure 7(a)/(b) and a wrench-like domain with two complex cavities as shown in Figure 7(c)/(d). The medial axes of these domains are computed and shown in Figures 7(a) and (c) while the corresponding curve skeletons are shown in Figures 7(b) and (d).

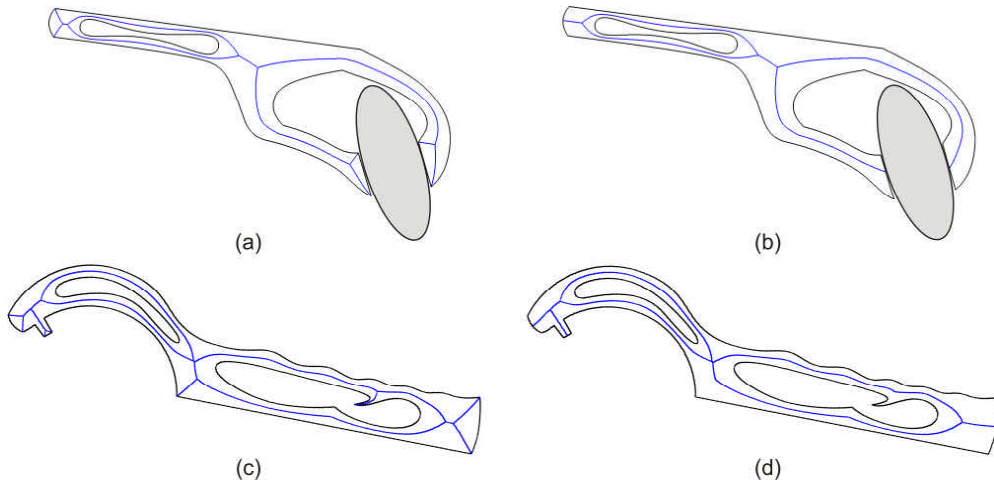


Fig. 7: A 2D cross-section of a compliant mechanism (robotic hand) and its medial axis (a) and curve skeleton (b); a wrench-like domain with two complex cavities and its medial axis (c) as well as its curve skeleton (d).

The distance function of a 2D section of a rotary cutter (a) and its medial axis (c) are illustrated in Figure 8. By modifying the distance functions of the nine outermost halfspaces, and substituting them into the R-function expression as explained in section 2, we obtain the continuous function shown in Figure 8(b). The final curve skeleton obtained after pruning is shown in Figure 8(d).

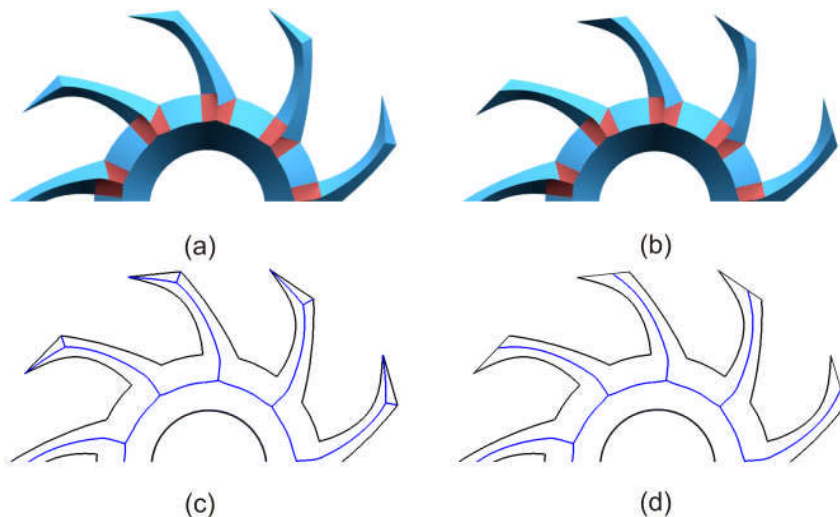


Fig. 8: A cross-section of a rotary cutter with its medial axis (c) and curve skeleton (d).



The final example of Figure 9 illustrates a domain containing two exponential sinusoidal primitives. The medial axis (Figure 9(c)) contains ten branches that are bounded by a junction point and a free end-point, and four that have a convex end-point at one end. Note that two rightmost branches are bounded by the same junction point and have convex end-point at the other end, but the two leftmost branches do not share the same junction point. Consequently, the distance function corresponding to the rightmost halfspace is modified as explained above so that the common junction point will move to the boundary of the domain. By eliminating all branches that are on the boundary of  $\Omega$  as well as all the other branches bounded by both a junction point as well as a free end-point, as explained in Section 3.1, we obtain the curve skeleton shown in Figure 9(e). Observe that the resulting curve skeleton intersects the boundary at only one point since the distance function corresponding to the leftmost halfspace has not been modified (see Figure 9(b)). Nevertheless, one can also modify the leftmost distance function for the domain of Figure 9(a) which will move the leftmost junction point to the boundary as shown in Figure 9(f).

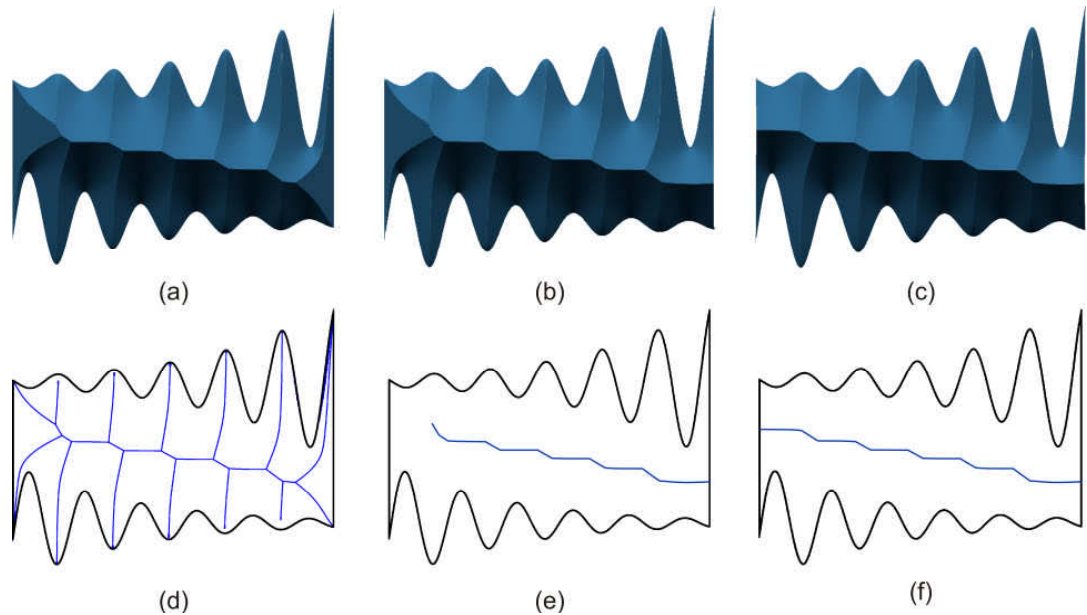


Fig. 9: An environment with two exponential sinusoidal primitives, its medial axis (c), and two curve skeletons (d) and (e) produced by the continuous functions shown in (a-c).

## 5 CONCLUSIONS

The concept of a curve skeleton has been used to capture the essential topologic and geometric properties of a shape, and there are many essentially ad-hoc definitions that treat them as “centerlines” or “medial curves”. Consequently, most existing definitions revolve around the (well-defined) concept of medial axis.

In this paper we propose a framework for computing curve skeletons of planar domains. Our formulation, which supports multiple criteria for defining curve skeletons, constructs exact distance functions with R-functions that operate on the real valued halfspaces bounding the domain as logic operators. We showed that curve skeletons can be obtained by: modifying specific halfspaces bounding the domain; substituting the modified halfspaces in the R-function expression; recomputing the corresponding skeleton, and by pruning specific branches of this modified skeleton.

We have also proposed one particular curve skeleton that is homeomorphic to the medial axis, and, hence, it preserves the homotopy of the domain by definition because the only branches that are pruned are those that have an end-point that does not connect to any other branches. Consequently, no internal loops of the medial axis are being affected. Furthermore, due to the pruning mechanisms

that we employ, the resulting skeleton is stable with respect to boundary noise even though the medial axis is not. At the same time, the proposed approach inherits all the computational advantages of our medial axis computation framework discussed in [25], whose mathematical apparatus is extendable to 3D domains, and has attractive computational properties, including the ability to implement it using standard algorithms within existing commercial CAD systems.

## ACKNOWLEDGMENTS

This work was supported in part by the National Science Foundation grants CMMI-0927105, CNS-0923158, CMMI-0555937, CAREER award CMMI-0644769, CMMI-0856401, and by a grant from Connecticut Center for Advanced Technology.

## REFERENCES

- [1] Blum, H.: A transformation for extracting new descriptions of shape. In *Models for the Perception of Speech and Visual Form*, 362-380, 1967.
- [2] Attali, D.; Boissonnat, J.-D.; Edelsbrunner, H.: Stability and computation of medial axis — a state-of-the-art report, In: Moller, T.; Hamann, B.; Russel, R.: (eds.), *Mathematical Foundations of Scientific Visualization, Computer Graphics, and Massive Data Exploration Mathematics and Visualization*, Springer Verlag, 2008.
- [3] Cornea, N.; Silver, D.; Min, P.: Curve-skeleton properties, applications, and algorithms. *IEEE Transactions on Visualization and Computer Graphics*, 13, 530-548, 2007.
- [4] Manzanera, A.; Bernard, T. M.; Longuet, B.: Medial faces from a concise 3D thinning algorithm. In *7th IEEE Conf. on Computer Vision*, pp. 337-343, 1999.
- [5] Borgefors, G.; Nyström, I.; Bajac, G. S. D.: Computing skeletons in three dimensions. *Pattern Recognition*, 32, 1225-1236, 1999. [doi:10.1016/S0031-3203\(98\)00082-X](https://doi.org/10.1016/S0031-3203(98)00082-X)
- [6] Rockett, P. I. An improved rotation-invariant thinning algorithm. *IEEE Trans. Pattern Anal. Mach. Intell.*, 27, 1671-1674, 2005. [doi:10.1109/TPAMI.2005.191](https://doi.org/10.1109/TPAMI.2005.191)
- [7] Attali, D.; Montanvert, A.: Computing and simplifying 2D and 3D continuous skeletons. *Comput. Vis. Image Underst.*, 67, 261-273, 1997. [doi:10.1006/cviu.1997.0536](https://doi.org/10.1006/cviu.1997.0536)
- [8] Bitter, I.; Kaufman, A. E.; Sato, M.: Penalized-distance volumetric skeleton algorithm. *IEEE Transactions on Visualization and Computer Graphics*, 7, 195-206, 2001.
- [9] Telea, A.; Vilanova, A.: A robust level-set algorithm for centerline extraction. *VISSYM '03: Proceedings of the symposium on Data visualisation*, Aire-la-Ville, Switzerland, Switzerland, pp. 185-194. Eurographics Association, 2003.
- [10] Sharf, A.; Lewiner, T.; Shamir, A.; Kobbelt, L.: On-the-fly curve-skeleton computation for 3D shapes. *Comput. Graph. Forum*, 26, 323-328, 2007. [doi:10.1111/j.1467-8659.2007.01054.x](https://doi.org/10.1111/j.1467-8659.2007.01054.x)
- [11] Arcelli, C.; di Baja, G. S.; Serino, L.: A parallel algorithm to skeletonize the distance transform of 3D objects. *Image and Vision Computing*, 27, 666 - 672, 2009. [doi:10.1016/j.imavis.2008.07.014](https://doi.org/10.1016/j.imavis.2008.07.014)
- [12] Hassouna, M. S.; Farag, A. A.: Robust centerline extraction framework using level sets. *Proceedings of the 2005 IEEE Computer Society Conference on Computer Vision and Pattern Recognition (CVPR'05) -Volume 1*, Washington, DC, USA, pp. 458-465. 2005.
- [13] Wu, F.; Ma, W.; Liou, P.; Laing, R.; Ouhyoung, M.: Skeleton extraction of 3D objects with visible repulsive force. In L. Kobbelt, H. H., P. Schröder (ed.), *Eurographics Symposium on Geometry Processing*, 2003.
- [14] Cornea, N.; Silver, D.; Yuan, X.; Balasubramanian, R.: Computing hierarchical curve-skeletons of 3D objects. *The Visual Computer*, 21, 945-955, 2005. [doi:10.1007/s00371-005-0308-0](https://doi.org/10.1007/s00371-005-0308-0)
- [15] Verroust, A.; Lazarus, F.: Extracting skeletal curves from 3D scattered data. *The Visual Computer*, 16, 15-25, 2000. [doi:10.1007/PL00007210](https://doi.org/10.1007/PL00007210)
- [16] Ferchichi, S.; Wang, S.; Grira, S.: New algorithm to extract centerline of 2D objects based on clustering. In *Image Analysis and Recognition*, Springer Berlin / Heidelberg, 364-374, 2007.
- [17] Bouix, S.; Siddiqi, K.; Tannenbaum, A.: Flux driven automatic centerline extraction. *Medical Image Analysis*, 9, 209-221, 2005. [doi:10.1016/j.media.2004.06.026](https://doi.org/10.1016/j.media.2004.06.026)

- [18] Dey, T. K.; Sun, J.: Defining and computing curve-skeletons with medial geodesic function. SGP '06: Proceedings of the fourth Eurographics symposium on Geometry processing, Aire-la-Ville, Switzerland, Switzerland, pp. 143-152. Eurographics Association, 2006.
- [19] Bauer, C.; Bischof, H.: Extracting curve skeletons from gray value images for virtual endoscopy. MIAR '08: Proceedings of the 4th international workshop on Medical Imaging and Augmented Reality, Berlin, Heidelberg, pp. 393-402. Springer-Verlag, 2008.
- [20] Zeng, J.; Lakaemper, R.; Yang, X.; Li, X.: 2D shape decomposition based on combined skeleton-boundary features. ISVC '08: Proceedings of the 4th International Symposium on Advances in Visual Computing, Part II, Berlin, Heidelberg, pp. 682-691. Springer-Verlag, 2008.
- [21] Donaghy, R. J.; Armstrong, C. G.; Price, M. A.: Dimensional reduction of surface models for analysis. *Engineering with Computers*, 16, 24-35, 2000. [doi:10.1007/s003660050034](https://doi.org/10.1007/s003660050034)
- [22] Suresh, K.: Automating the CAD/CAE dimensional reduction process. SM '03: Proceedings of the eighth ACM symposium on Solid modeling and applications, pp. 76-85. ACM, New York, NY, USA, 2003.
- [23] Sundar, H.; Silver, D.; Gagvani, N.; Dickinson, S.: Skeleton based shape matching and retrieval. SMI '03: Proceedings of the Shape Modeling International 2003, Washington, DC, USA 130. IEEE Computer Society, 2003.
- [24] Wan, M.; Dachille, F.; Kaufman, A.: Distance-field based skeletons for virtual navigation. *Proc. Visualization VIS '01*, pp. 239-560, 2001.
- [25] Eftekharian, A. A.; Ilies, H. T.: Distance functions and skeletal representations of rigid and non-rigid planar shapes. *Computer-Aided Design*, 41, 865 - 876, 2009. [doi:10.1016/j.cad.2009.05.006](https://doi.org/10.1016/j.cad.2009.05.006)
- [26] Pottmann, H.; Hofer, M.: Geometry of the squared distance function to curves and surfaces. *Visualization and Mathematics III*, 221-245, Springer 2002.
- [27] Sud, A.; Govindaraju, N.; Gayle, R.; Andersen, E.; Manocha, D.: Surface distance maps. *Proceedings of Graphics Interface*, New York, NY, USA, pp. 35-42. ACM, 2007.
- [28] Rvachev, V.; Sheiko, T.: R-functions in boundary value problems in mechanics. *Applied Mechanics Reviews*, 48, 151-186, 1995. [doi:10.1115/1.3005099](https://doi.org/10.1115/1.3005099)
- [29] Shapiro, V.: Semi-analytic geometry with R-functions. *Acta Numerica*, 18, 239-303, 2007.
- [30] Dobkin, D.; Guibas, L.; Hershberger, J.; Snoeyink, J.: An efficient algorithm for finding the CSG representation of a simple polygon. SIGGRAPH '88: Proceedings of the 15th annual conference on Computer graphics and interactive techniques, New York, NY, USA, pp. 31-40. ACM, 1988.
- [31] Shapiro, V.: A convex deficiency tree algorithm for curved polygons. *Int. J. Computational Geometry and Applications*, 11, 215-238, 2001.
- [32] Shapiro, V.: Theory of R-functions and applications: A primer. Technical Report TR91-1219. Computer Science Department, Cornell University, Ithaca, NY, 1991.
- [33] Buchele, S. F.; Crawford, R. H.: Three-dimensional halfspace constructive solid geometry tree construction from implicit boundary representations. *Proceedings of the 8th ACM Symposium on Solid Modeling and Applications*, 135-144. ACM Press, 2003.
- [34] Choi, H. I.; Choi, S. W.; Moon, H. P.: Mathematical theory of medial axis transform. *Pacific Journal of Mathematics*, 1, 57-88, 1997. [doi:10.2140/pjm.1997.181.57](https://doi.org/10.2140/pjm.1997.181.57)
- [35] Sherbrooke, E. C.; Patrikalakis, N. M.; Wolter, F.: Differential and topological properties of medial axis transforms. *Graph. Models Image Process.*, 58, 574-592, 1996. [doi:10.1006/gmip.1996.0047](https://doi.org/10.1006/gmip.1996.0047)